Electronic Supplementary Material (ESI) for New Journal of Chemistry.

Supporting Information For:

Carbazole modified salicylaldimines and the difluoroboron complexes: effect of the terminal groups of *tert*-butyl and trifluoromethyl on the organogelation and piezofluorochromism

Table S1. Photophysical data of componds **1a**-**3a** and their complexes **1b**-**3b**.

Compound	Solvents	λ_{abs}^{max}/nm	λ_{em}/nm	Stokes shift[a]/nm	Φ_F[b]
1a	Cyclohexane	371	550	179	< 0.01
	Toluene	370	551	181	< 0.01
	Ethyl acetate	363	550	187	< 0.01
	Chloroform	369	548	179	< 0.01
	Dichloromethane	366	550	184	< 0.01
2a	Cyclohexane	375	569	194	< 0.01
	Toluene	376	569	193	< 0.01
	Ethyl acetate	368	580	212	< 0.01
	Chloroform	375	579	204	< 0.01
	Dichloromethane	375	583	208	< 0.01
3a	Cyclohexane	383	550	167	< 0.01
	Toluene	381	552	171	< 0.01
	Ethyl acetate	370	549	179	< 0.01
	Chloroform	378	551	173	< 0.01
	Dichloromethane	375	550	175	< 0.01
1b	Cyclohexane	400	494, 517	94	0.15
	Toluene	399	535	136	0.19
	Ethyl acetate	387	586	199	0.02
	Chloroform	405	577	172	0.09
	Dichloromethane	401	605	204	0.01

2b	Cyclohexane	395	502, 526	107	0.11
	Toluene	412	532	120	0.25
	Ethyl acetate	397	588	191	0.01
	Chloroform	416	599	183	0.03
	Dichloromethane	412	615	203	< 0.01
3b	Cyclohexane	428	514, 543	86	0.22
	Toluene	415	563	148	0.16
	Ethyl acetate	395	607	212	<0.01
	Chloroform	418	621	203	< 0.01

[a] Calculated from the difference of λ_{em} and λ_{abs}^{max}.

[b] Fluorescence quantum yields were determined by a standard method with diphenylanthracene in benzene ($\Phi_F = 0.85$, λ_{ex} = 390 nm) as reference.

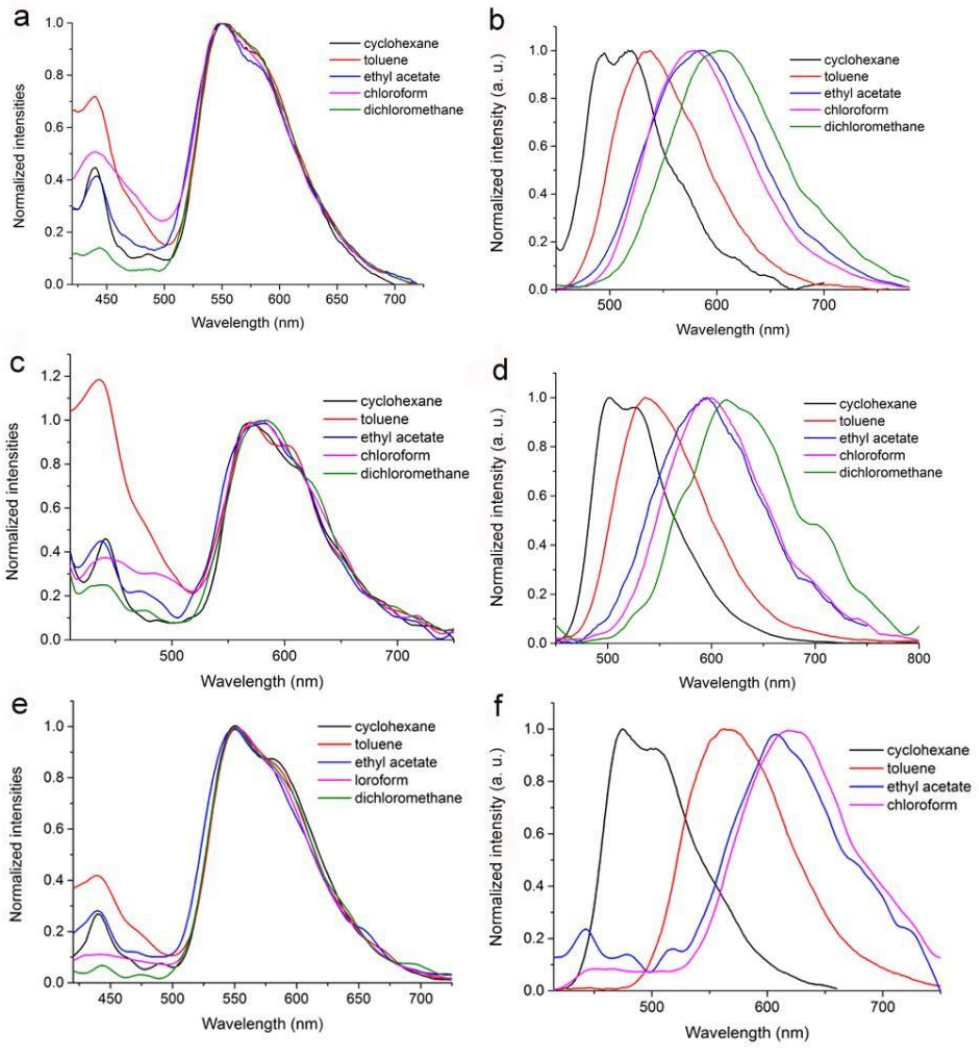

Fig. S1 Normalized fluorescence emission spectra of **1a** (a), **1b** (b), **2a** (c), **2b** (d), **3a** (e) **and 3b** (f) in different solvents (1.0×10^{-5}M, λ_{ex} = 390 nm).

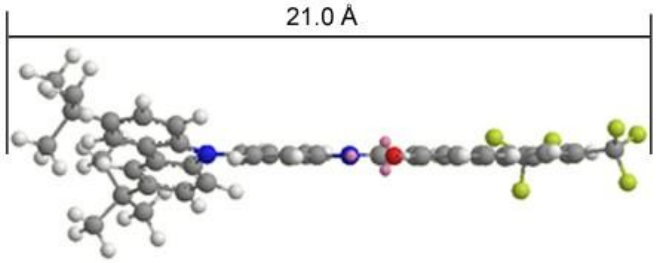

Fig. S2 The optimized configurations for **3a** calculated by the **DFT** method (B3LYP/6-31G level) on Gaussian 09 software.

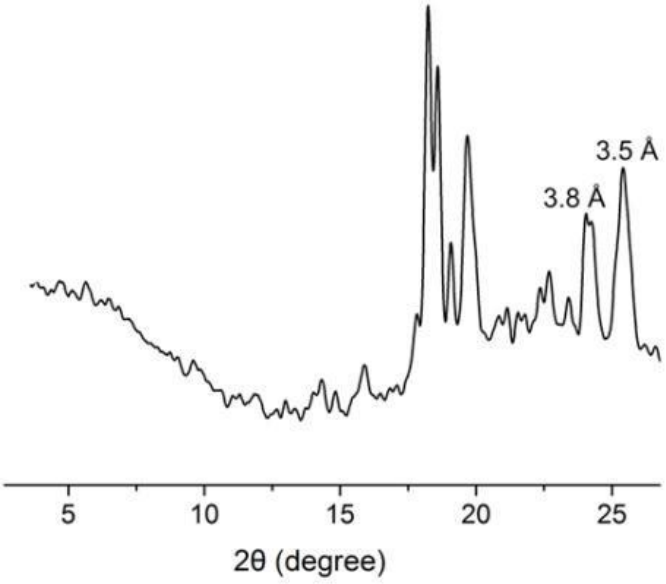

Fig. S3 XRD pattern of xerogel **3b** obtained from cyclohexane.

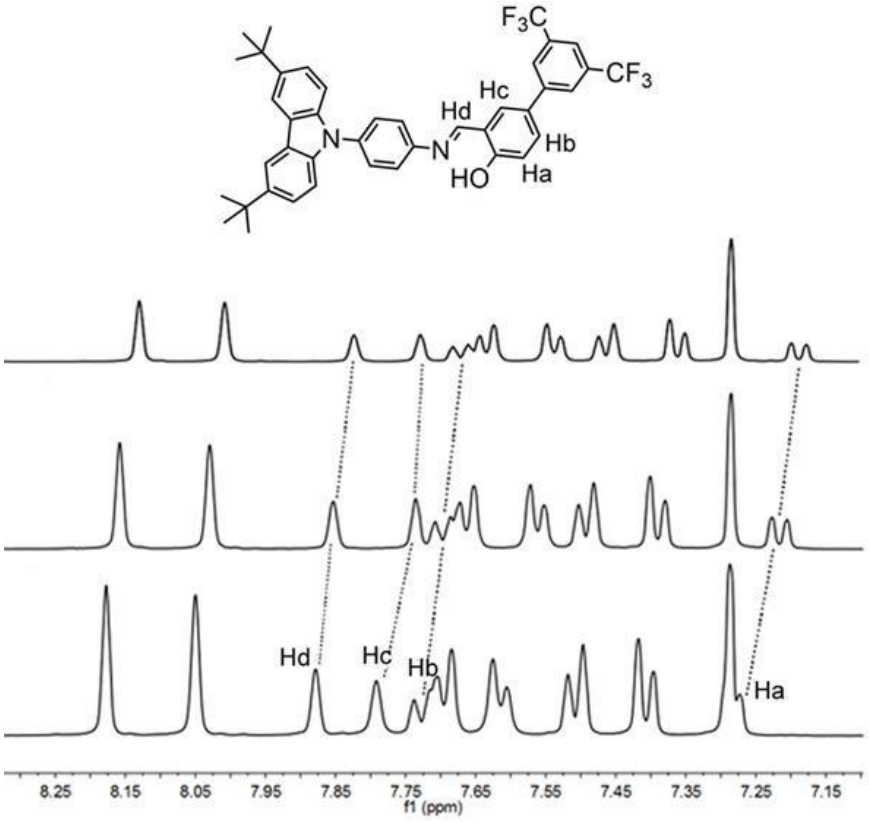

Fig. S4 ^{1}H NMR spectra of **3a** in the absence (a) as well as in the presence of 1.0 equiv. (b) and 2.0 equiv. (c) of TBAF.

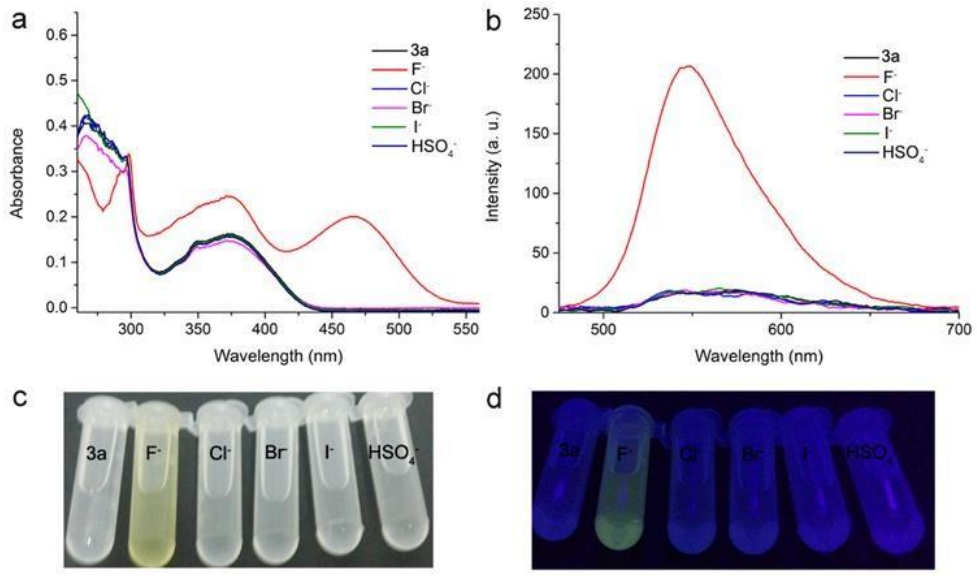

Fig. S5 UV-vis absorption (a) and fluorescence emission (b, λ_{ex} = 380 nm) spectra of **3a** (1.0×10^{-5} M) in the presence of various tetrabutylammonium anions (4 equiv.) in THF; Photos of **3a** in THF in the presence of 4 equiv. anions under daylight (c) and UV irradiation at 365 nm (d).

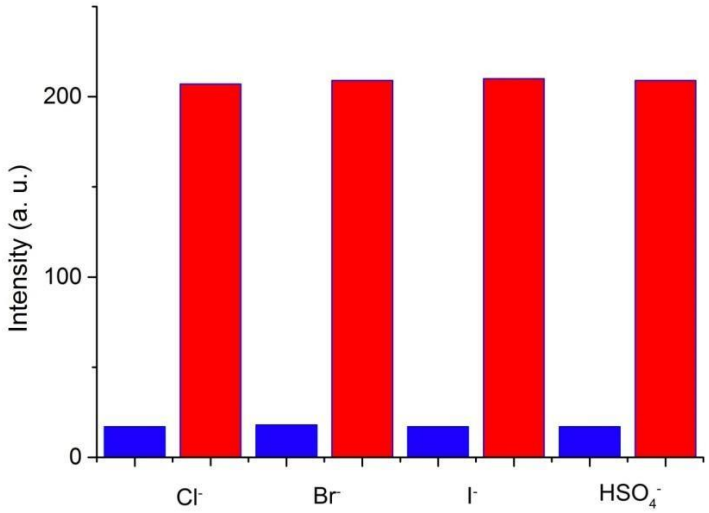

Fig. S6 Fluorescence intensity at 567 nm for **3a** (1.0×10^{-5} M) in THF upon the addition of 4 equiv. of Cl^-, Br^-, I^- and HSO_4^- (blue bar, from left to right) and fluorescence intensity at 567 nm for **3a** (1.0×10^{-5} M) in THF upon the addition of 4 equiv. of F^- in presence of 4 equiv. of Cl^-, Br^-, I^- and HSO_4^- (red bar, from left to right).

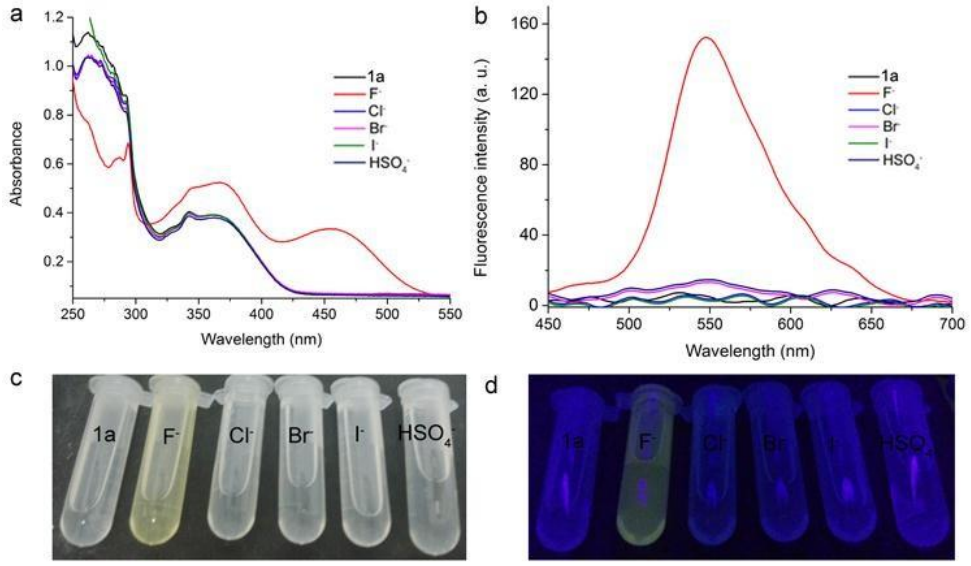

Fig. S7 UV-vis absorption (a) and fluorescence emission (b, λ_{ex} = 390 nm) spectra of **1a** (1.0×10^{-5} M) in the presence of various tetrabutylammonium anions (4 equiv.) in THF; Photos of **1a** in THF in the presence of 4 equiv. anions under daylight (c) and UV irradiation at 365 nm (d).

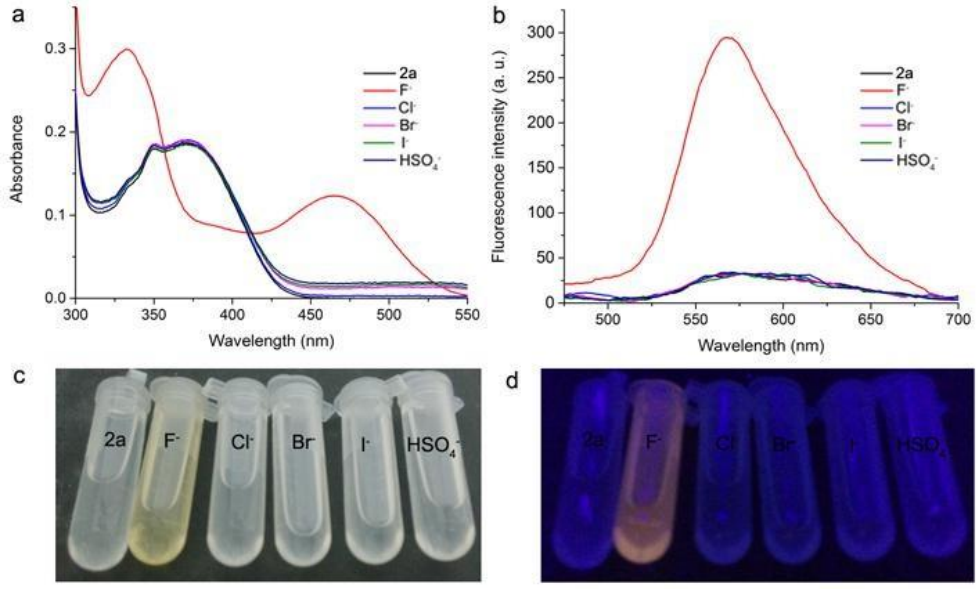

Fig. S8 UV-vis absorption (a) and fluorescence emission (b, λ_{ex} = 410 nm) spectra of **2a** (1.0×10^{-5} M) in the presence of various tetrabutylammonium anions (4 equiv.) in THF; Photos of **2a** in THF in the presence of 4 equiv. anions under daylight (c) and UV irradiation at 365 nm (d).

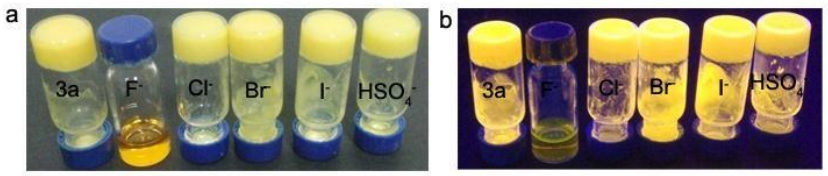

Fig. S9 Photos of organogel **3a** in *n*-heptane in the presence of 4 equiv. anions under daylight (a) and UV irradiation at 365 nm (b).

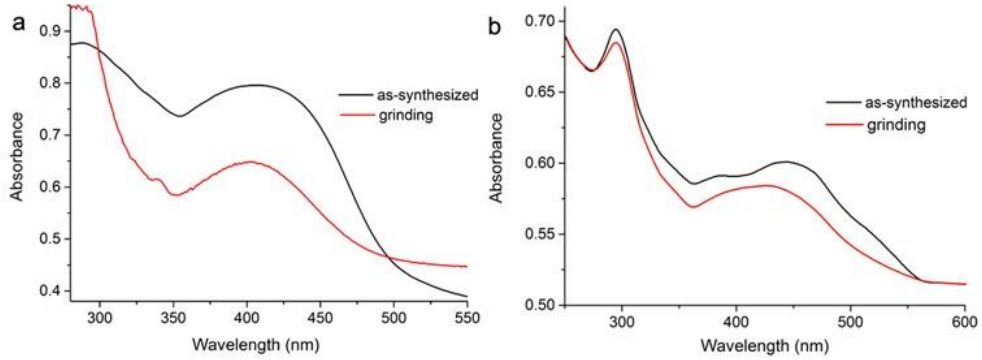

Fig. S10 UV-vis spectra of **1b** (a) and **3b** (b) in as-prepared crystal and ground powders.

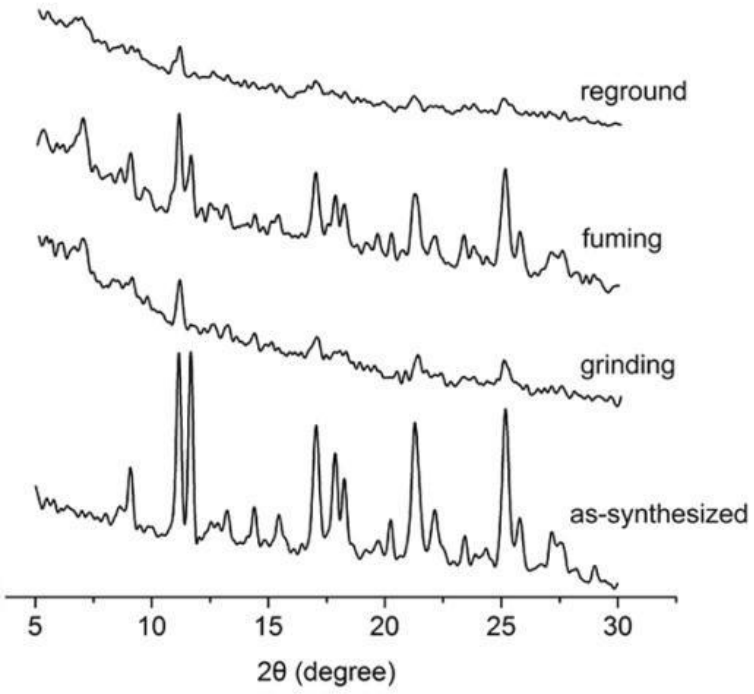

Fig. S11 XRD patterns of compound **1b** in different solid states.

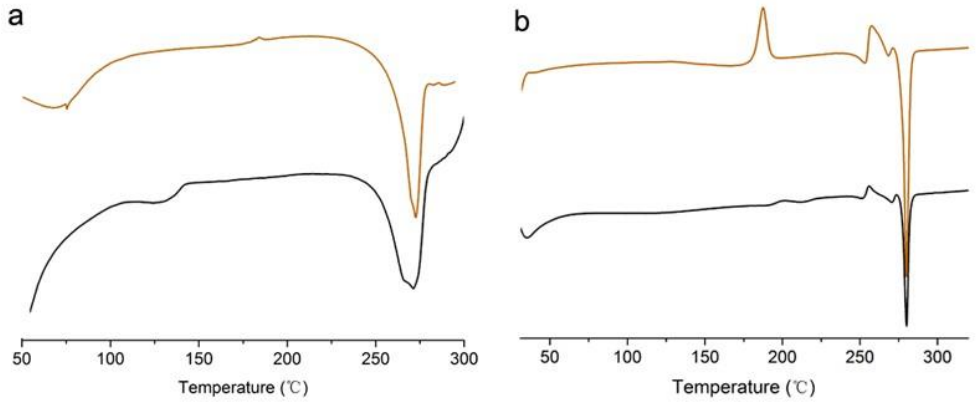

Figure S12. DSC thermograms of **1b** (a) and **3b** (b) in as-prepared crystal (black line) and ground powder (red line) under nitrogen atmosphere at a heating rate of 10 °C/min.

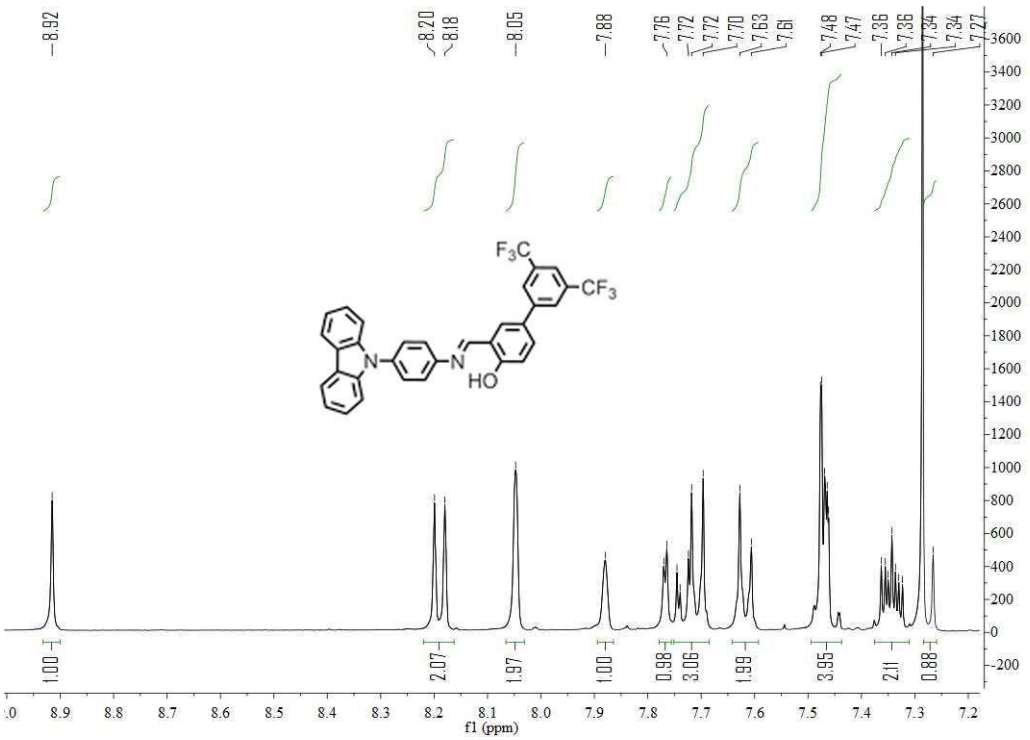

Fig. S13 ^{1}H NMR (400 MHz, $CDCl_3$) spectrum of **1a**.

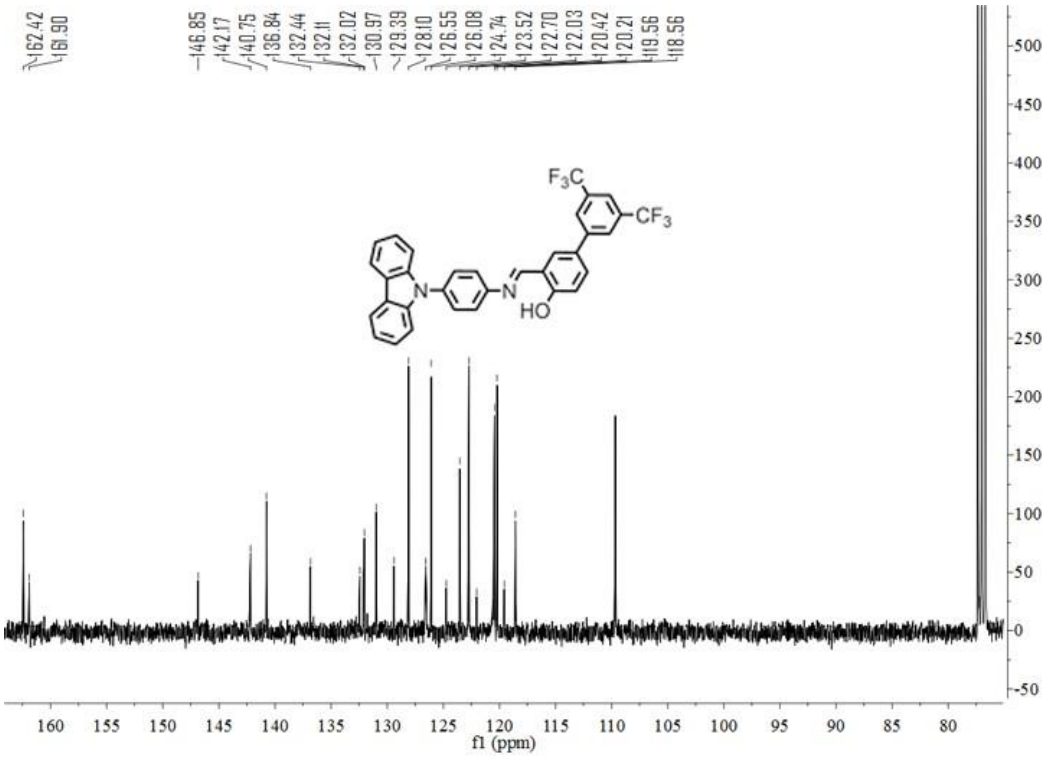

Fig. S14 ^{13}C NMR (100 MHz, $CDCl_3$) spectrum of **1a**.

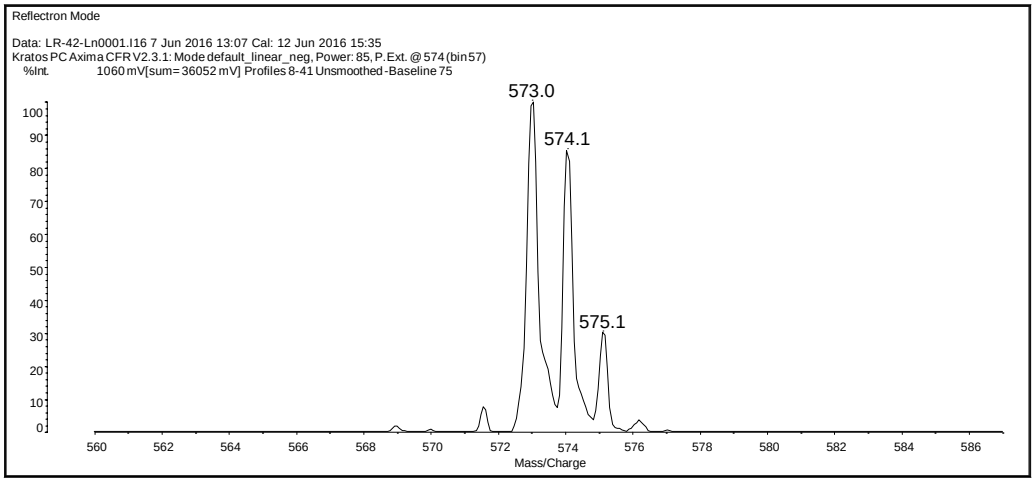

Fig. S15 MALDI/TOF MS spectrum of **1a**.

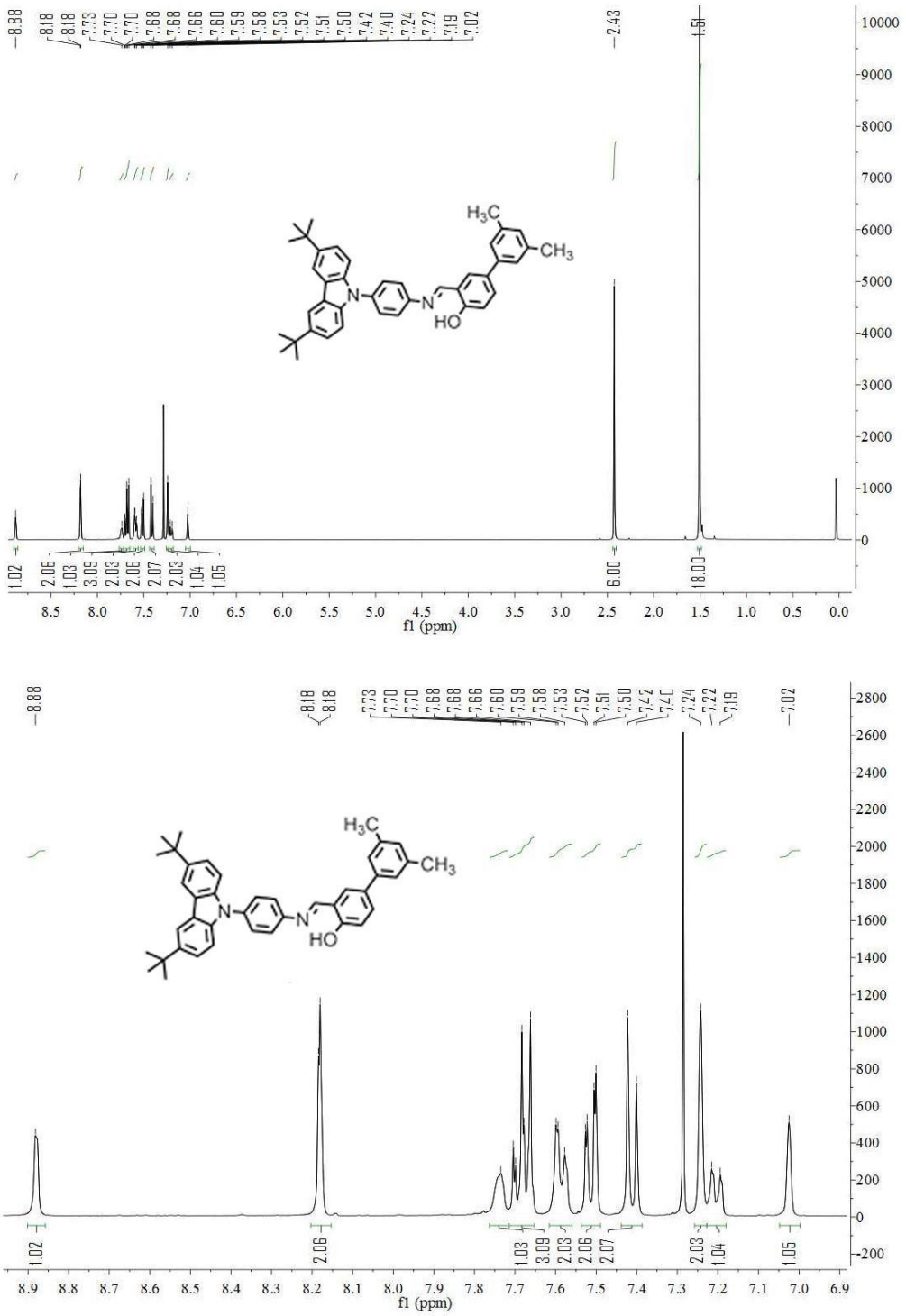

Fig. S16 ^{1}H NMR (400 MHz, $CDCl_3$) spectrum of **2a**.

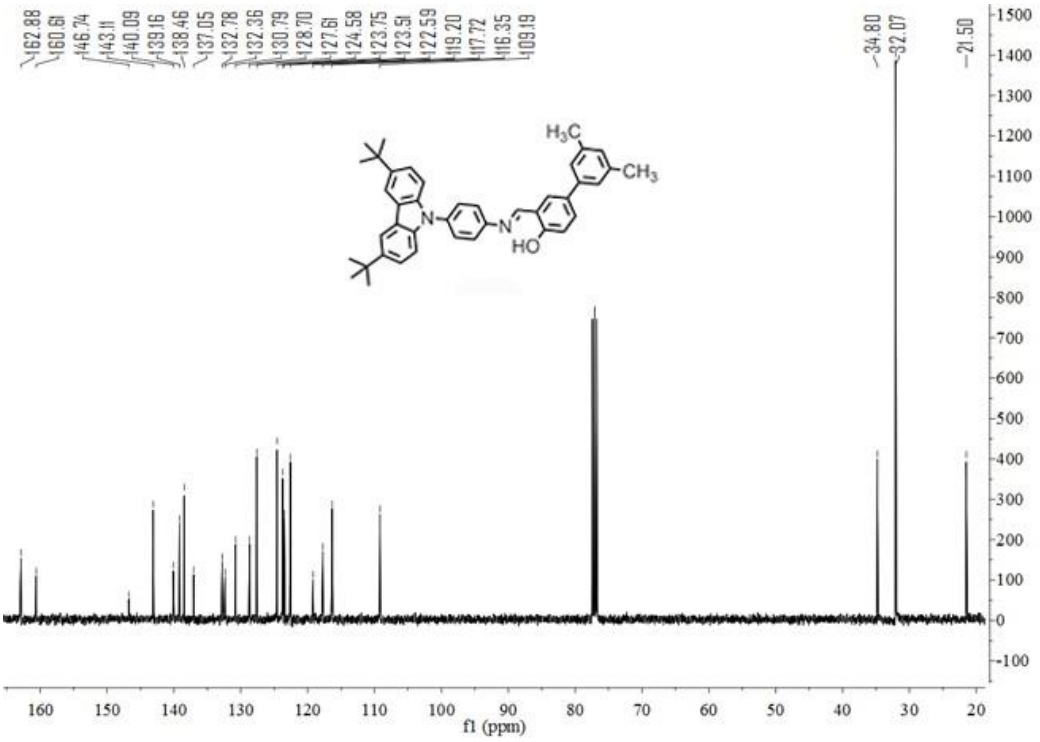

Fig. S17 ^{13}C NMR (100 MHz, $CDCl_3$) spectrum of **2a**.

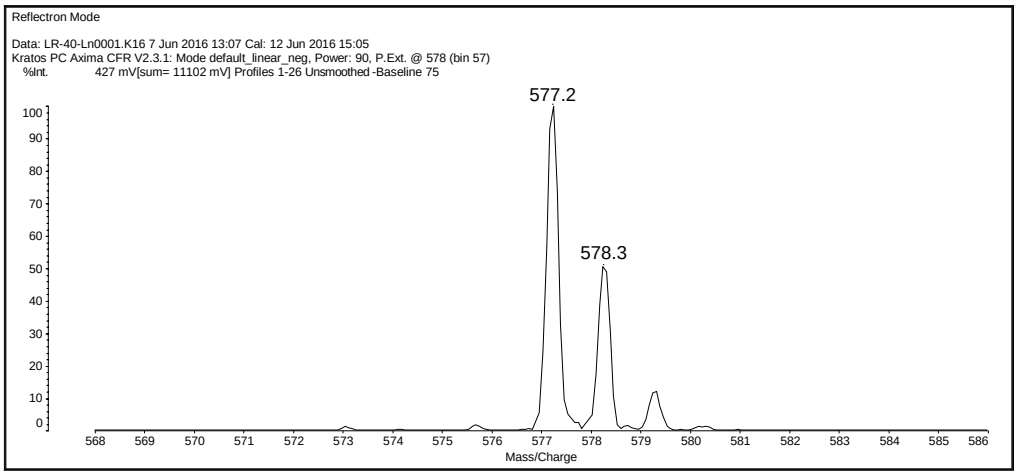

Fig. S18 MALDI/TOF MS spectrum of **2a**.

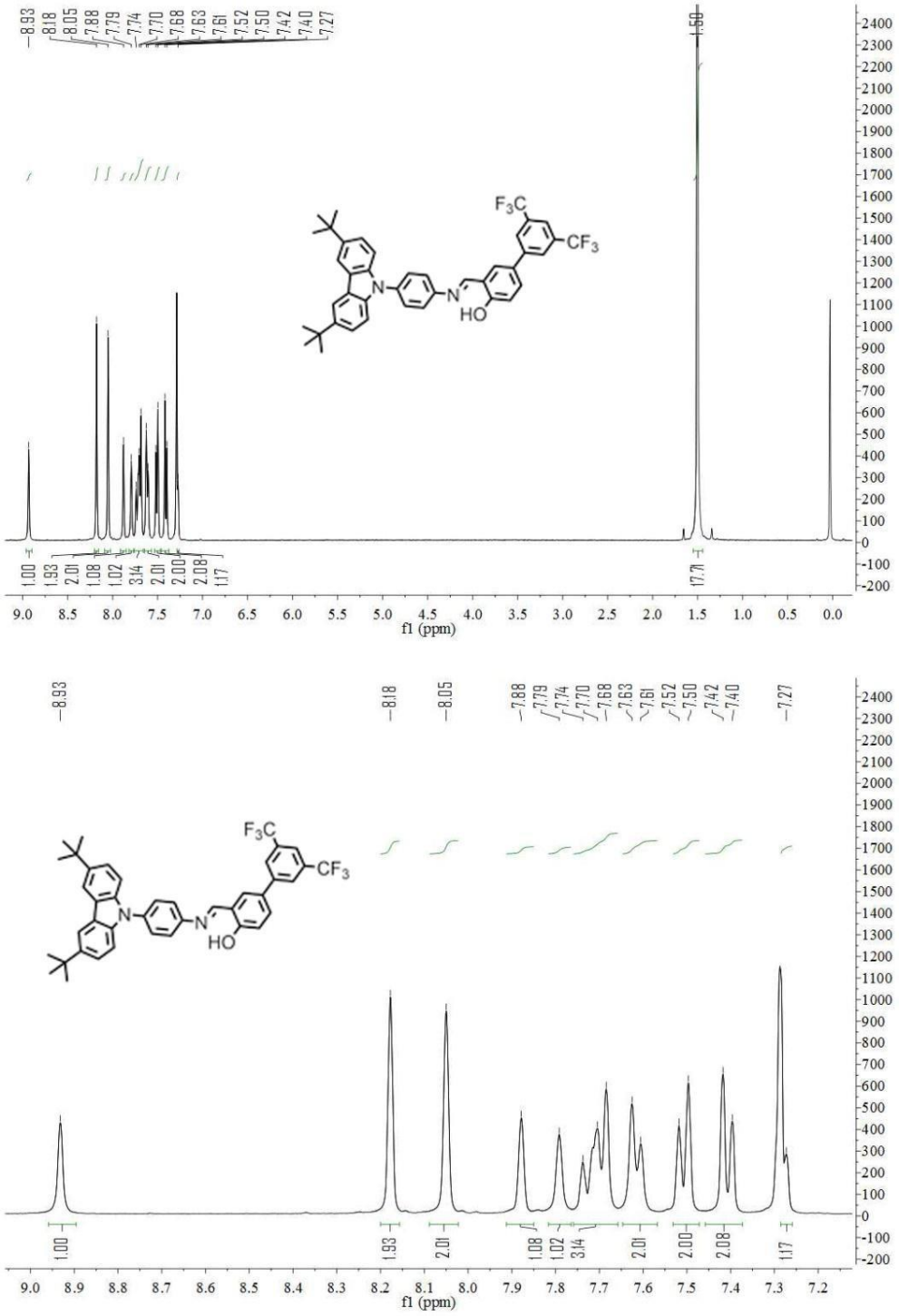

Fig. S19 ^{1}H NMR (400 MHz, $CDCl_3$) spectrum of **3a**.

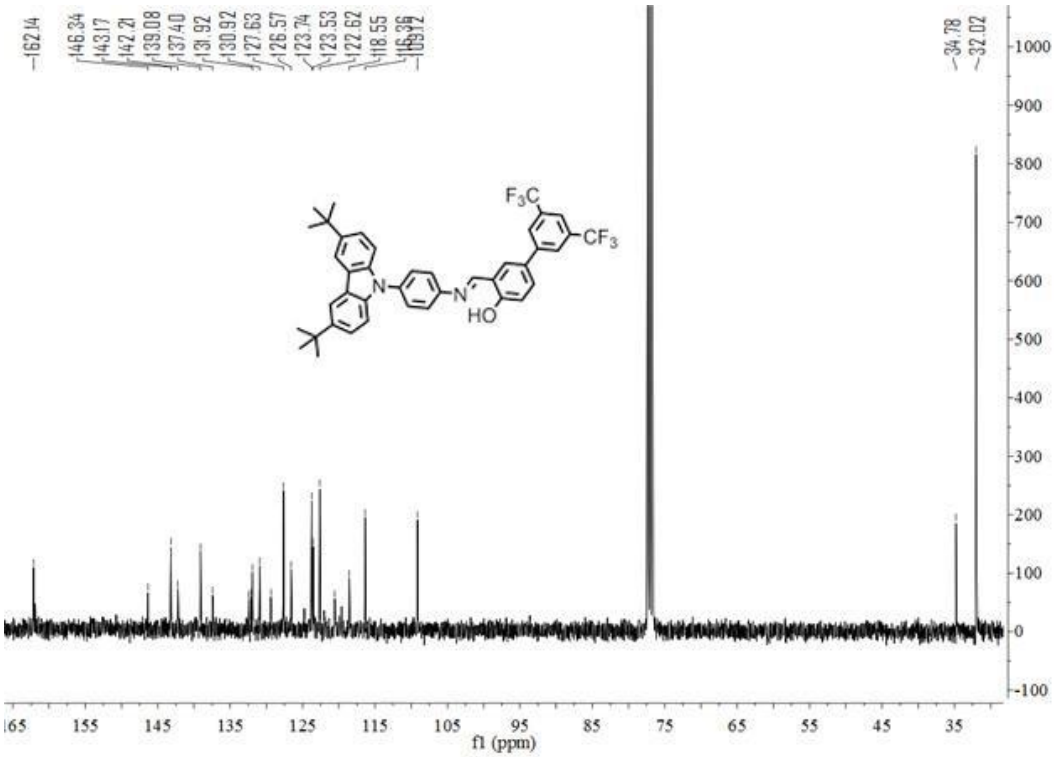

Fig. S20 ^{13}C NMR (100 MHz, $CDCl_3$) spectrum of **3a**.

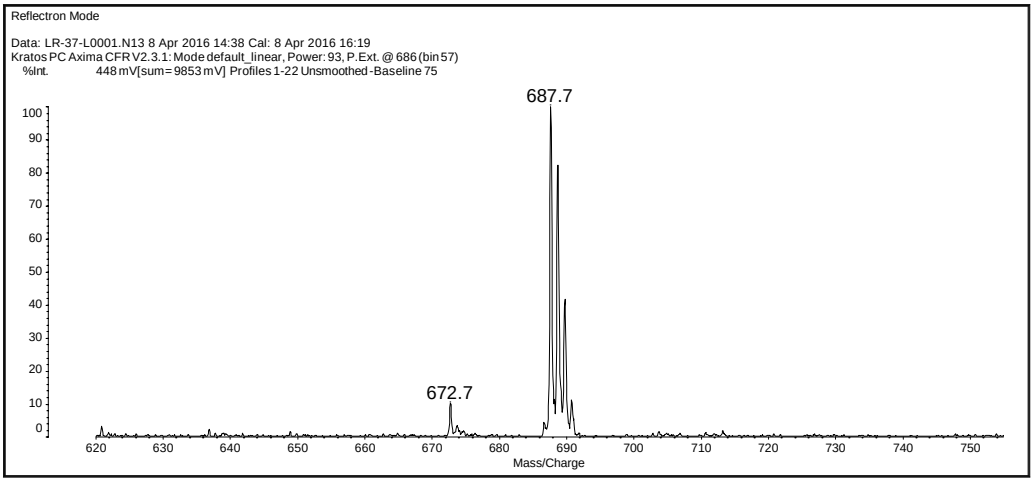

Fig. S21 MALDI/TOF MS spectrum of **3a**.

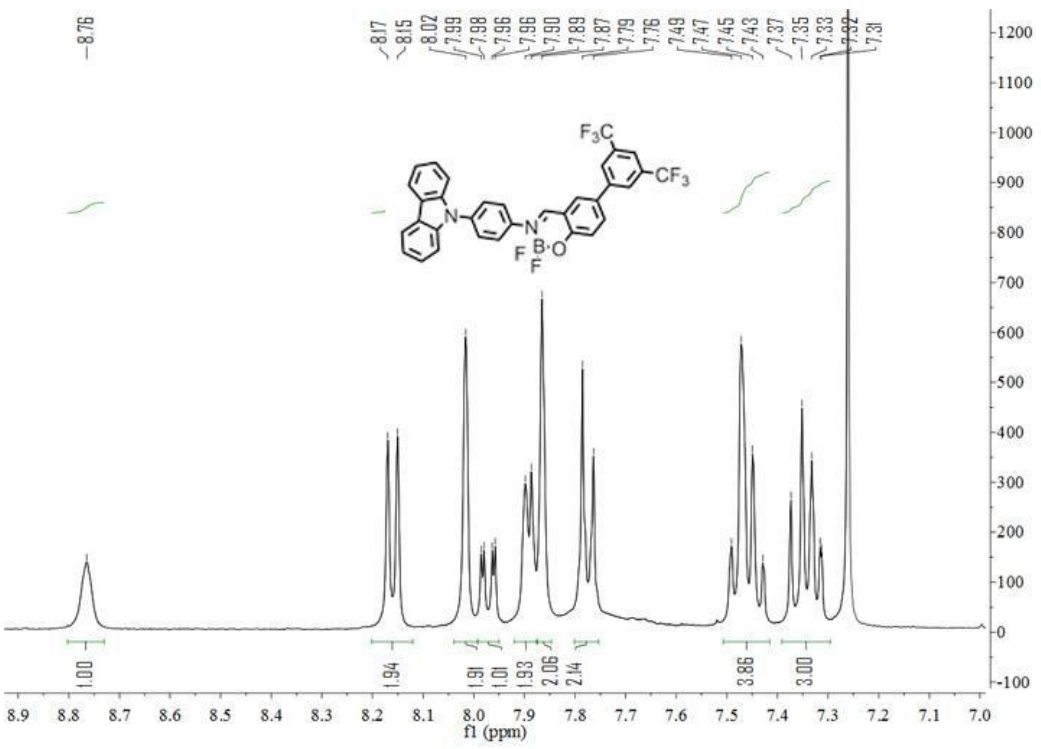

Fig. S22 ^{1}H NMR (400 MHz, $CDCl_3$) spectrum of **1b**.

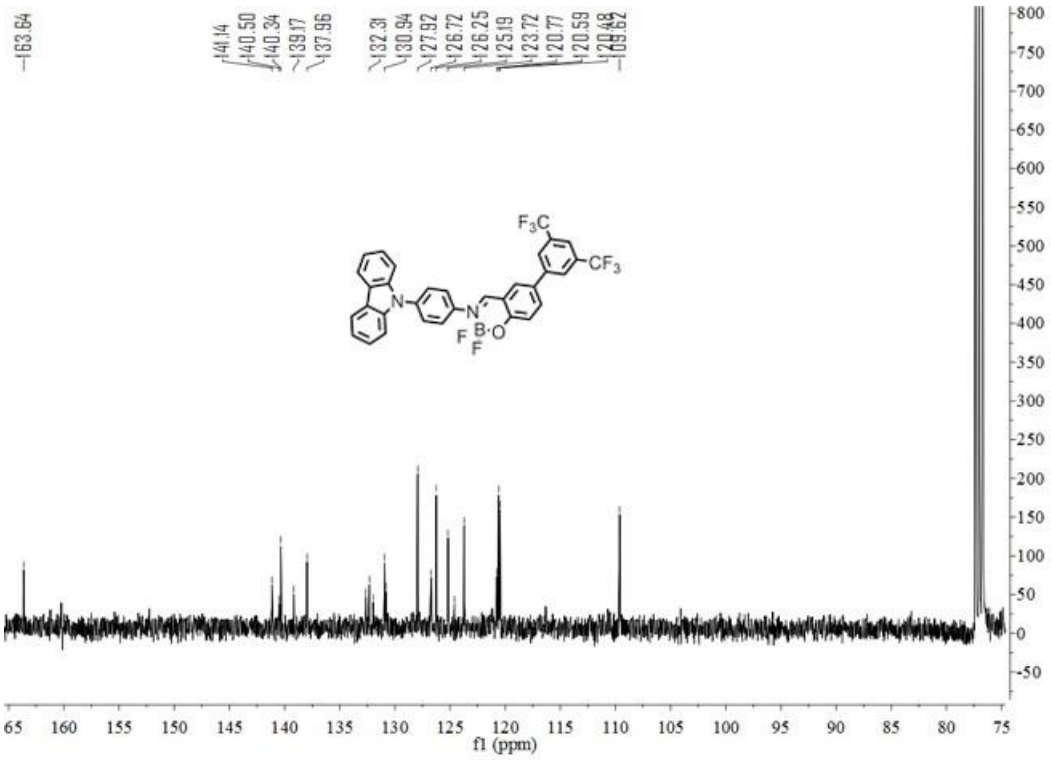

Fig. S23 ^{13}C NMR (100 MHz, $CDCl_3$) spectrum of **1b**.

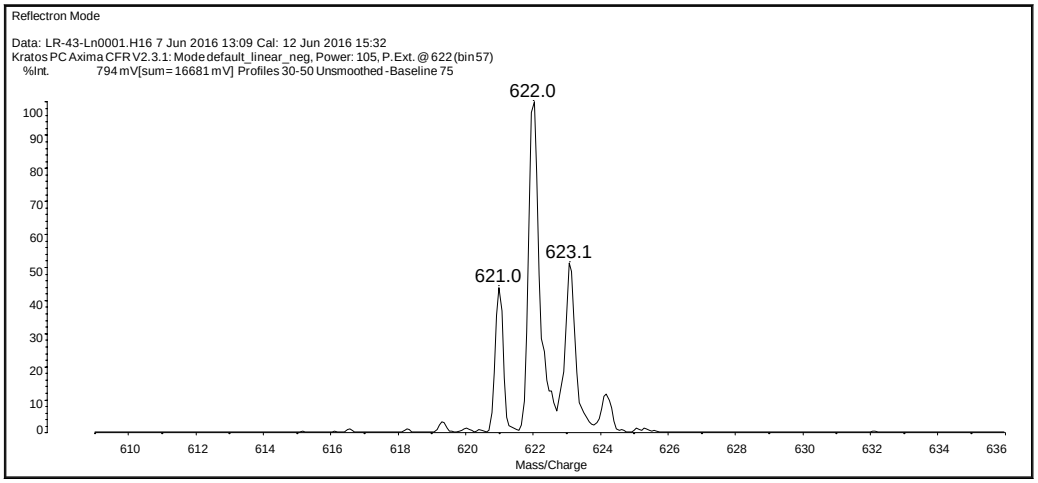

Fig. S24 MALDI/TOF MS spectrum of **1b**.

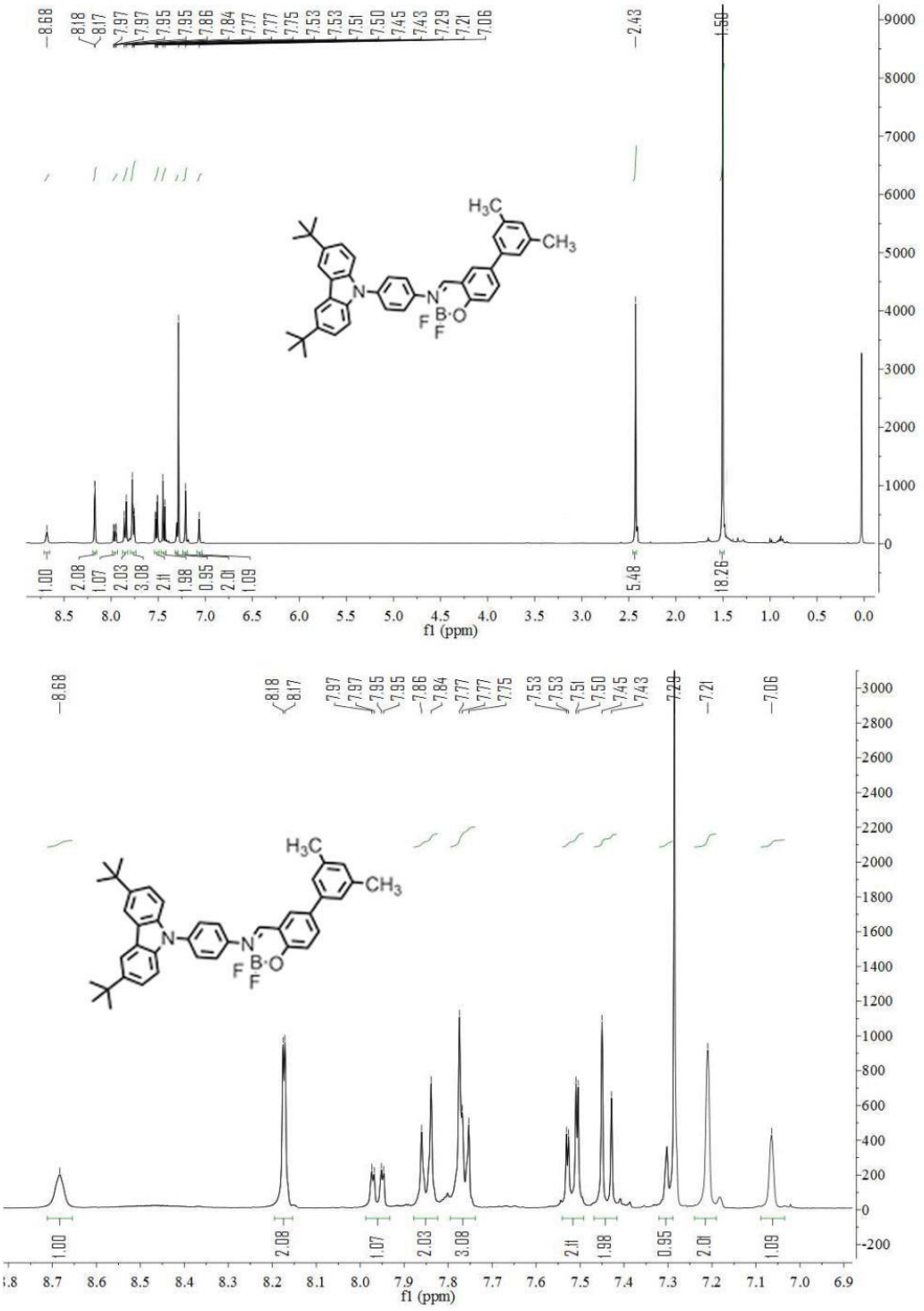

Fig. S25 ^{1}H NMR (400 MHz, $CDCl_3$) spectrum of **2b**.

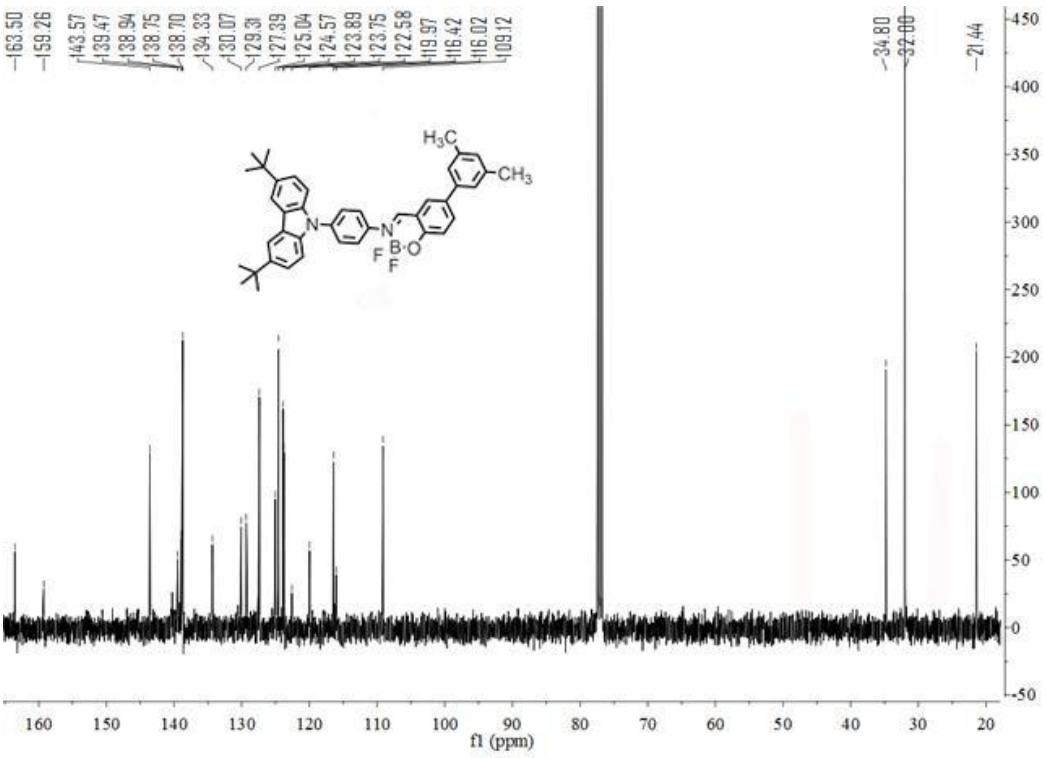

Fig. S26 ^{13}C NMR (100 MHz, $CDCl_3$) spectrum of **2b**.

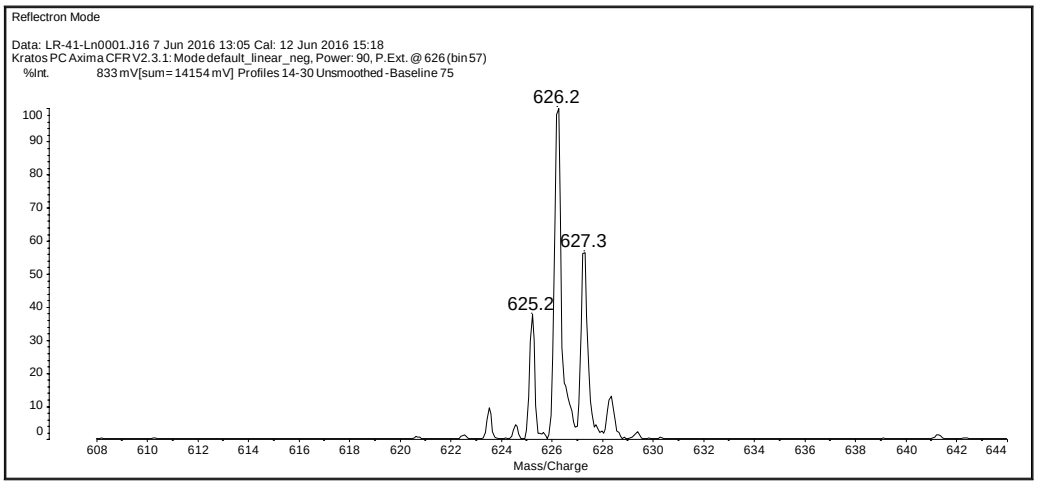

Fig. S27 MALDI/TOF MS spectrum of **2b**.

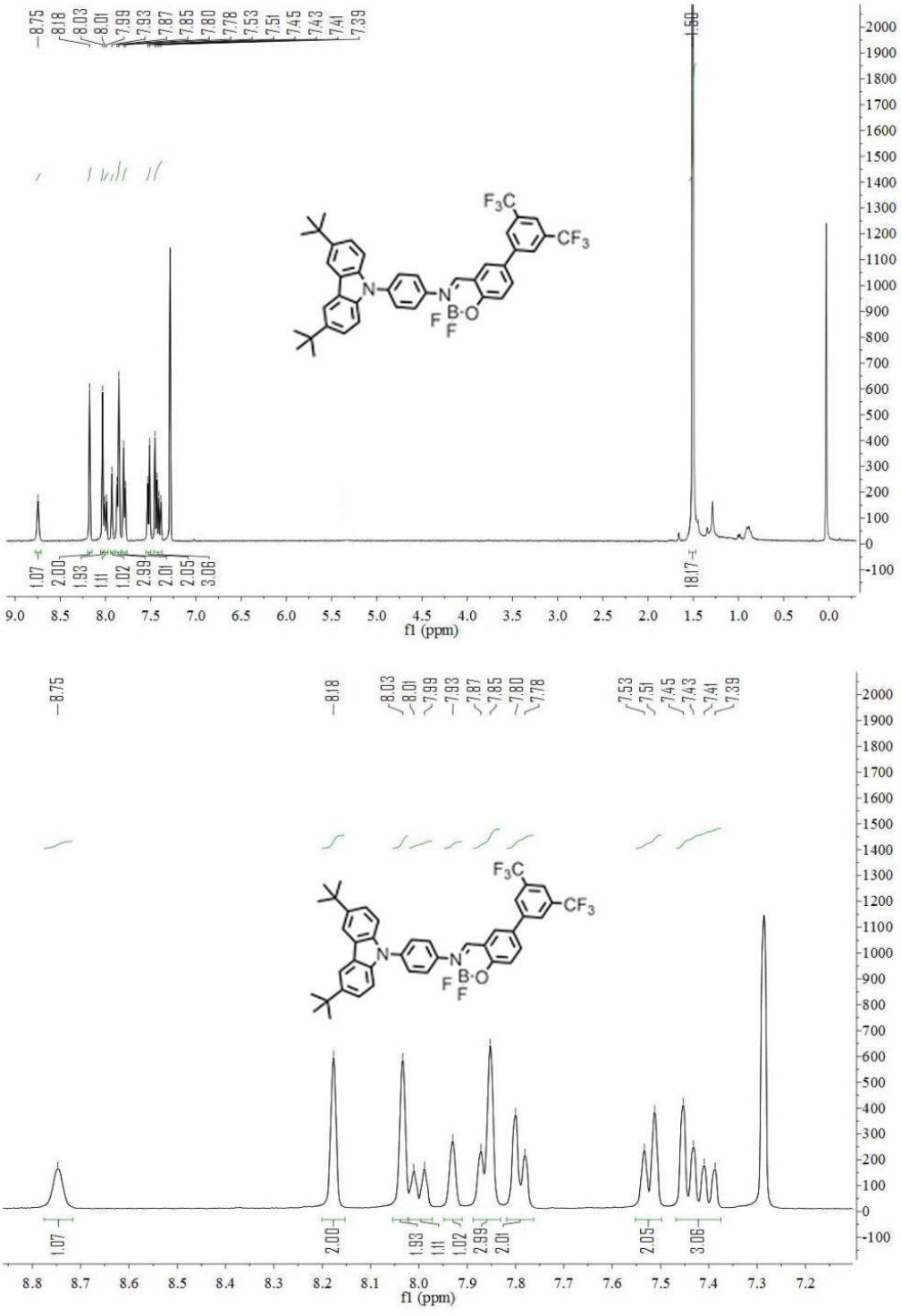

Fig. S28 ^{1}H NMR (400 MHz, $CDCl_3$) spectrum of **3b**.

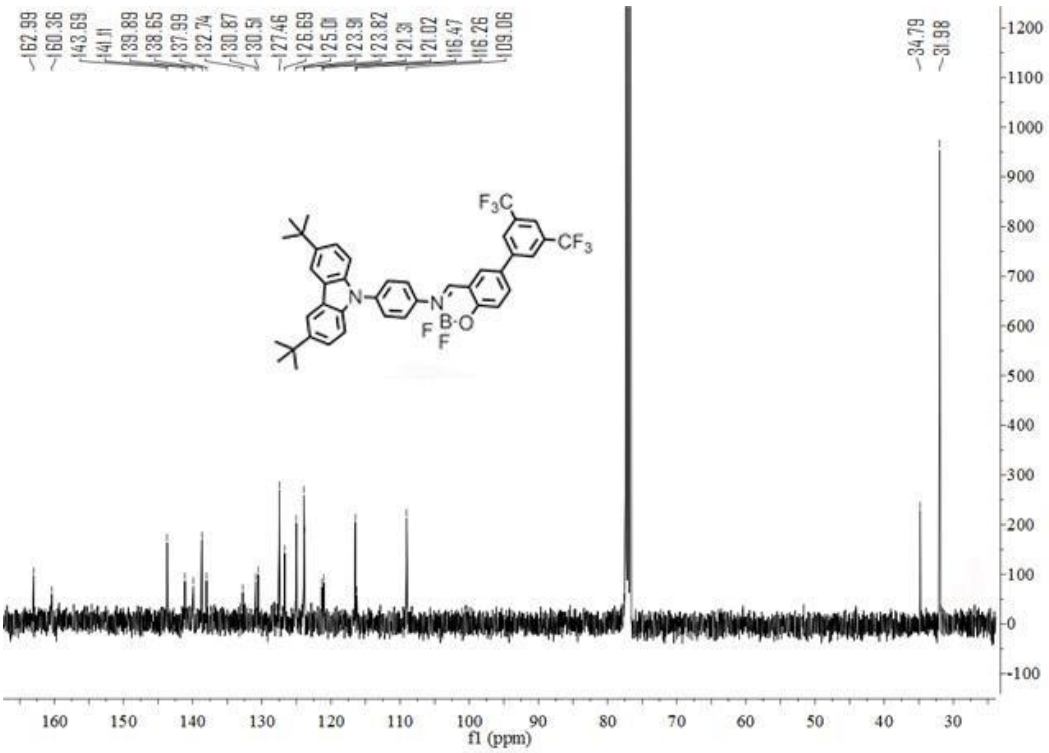

Fig. S29 ^{13}C NMR (100 MHz, $CDCl_3$) spectrum of **3b**.

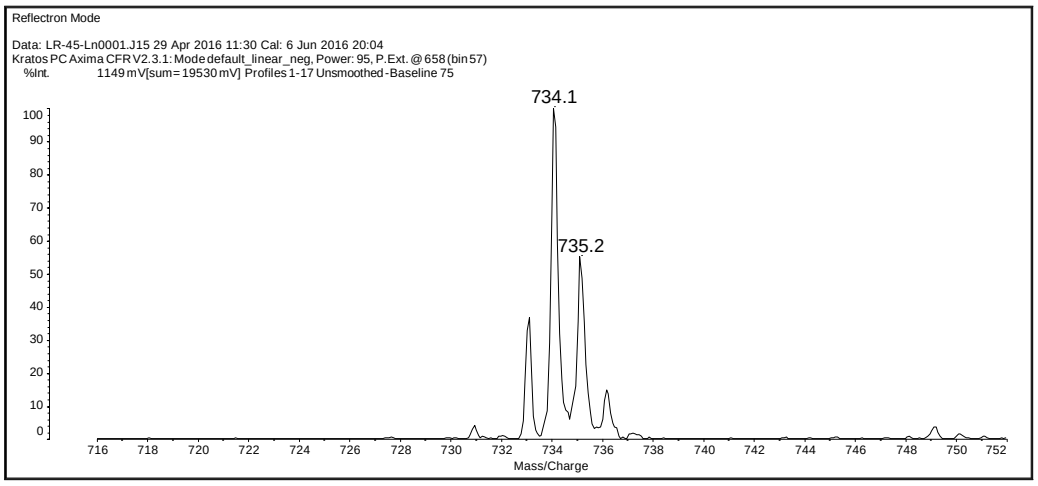

Fig. S30 MALDI/TOF MS spectrum of **3b**.